JCTC Journal of Chemical Theory and Computation
Letter
pubs.acs.org/JCTC

A Natural Helical Crystal Lattice Model for Carbon Nanotubes

Elise Y. Li*,† and Nicola Marzari*,‡

†Department of Chemistry, National Taiwan Normal University, Taipei, Taiwan 11677

‡Theory and Simulations of Materials (THEOS), École Polytechnique Fédérale de Lausanne, CH-1015 Lausanne, Switzerland

Supporting Information

ABSTRACT: We propose a novel helical crystal lattice model for chiral and achiral carbon nanotubes (CNTs) where the unit cell and the helical crystal vector are defined in a unique and systematic manner for arbitrary CNTs. The small unit cell of this helical crystal lattice leads to a natural and convenient description of the electronic structure of chiral CNTs. Also, using this model, the degenerate frontier Bloch wave functions at the Γ point can be conveniently chosen by their symmetry properties. In particular, the contour of the Bloch wave functions at the Fermi level can be easily predicted for all metallic CNTs.

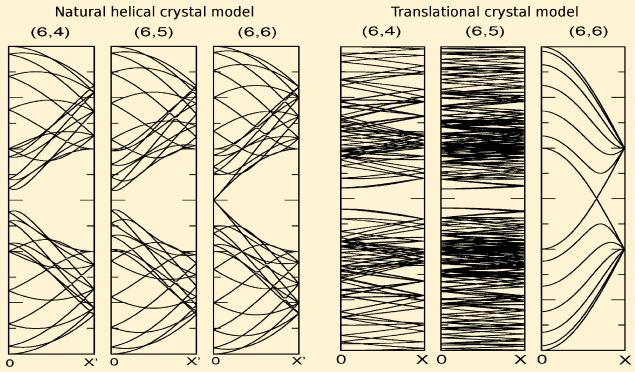

Single-walled carbon nanotubes (SWCNTs) can be formed by rolling up a graphene sheet into a cylinder. The geometry of a CNT, depending on the way the graphene sheet is wrapped, can be completely specified by a pair of integers (n, m), or by the radius R and the chiral angle θ of the nanotube.[1,2] The electronic properties of CNTs are highly sensitive to their structure, and CNTs can be either metallic (when $n - m = 3l$, $l = 0, 1, 2, 3...$) or semiconducting (when $n - m = 3l \pm 1$). Typically, the electronic structure of a CNT is studied within periodic boundary conditions. For achiral CNTs, i.e. armchair (n,n)-CNTs or zigzag $(n,0)$-CNTs, the translational unit cell is small and contains only $4n$ carbon atoms. However, in cases of chiral CNTs, the minimal translational unit cell often contains a large number of atoms even for nanotubes with small diameters. Due to this reason, most theoretical studies on CNTs are limited to armchair or zigzag types, and there have been no systematic studies on the electronic properties for chiral CNTs.

Alternatively, given that a chiral nanotube has a helical structure, it may be more naturally described by a helical crystal lattice. Helical systems such as DNA strands or α-helix proteins possess screw symmetry, and their electronic structure may be equivalently described using the smallest screw displacement $S(\phi,\tau)$ as the elementary operation.[3] In general, the primitive translation $\mathbf{T}$ for a helical system can be decomposed into n-fold repeats of the screw operation around an axis parallel to $\mathbf{T}$, i.e., $\mathbf{T}(t) = \mathbf{S}^n(\phi,\tau)$, where $\mathbf{T}(t)$ is the translation by t and $\mathbf{S}(\phi,\tau)$ is the screw operation that consists of a translation by τ followed by a rotation by ϕ (the vectors t, τ, and ϕ are related by $n = t/\tau = 2\pi i/\phi$, where i is an integer). Then, the overall structure of a helical system can also be generated by a screw axis operation on a smaller unit cell around the principal axis; i.e., the straight translational vector $\mathbf{T}$ can be replaced by a helical (geodesic) vector $\mathbf{T}_R$. While the extension of $\mathbf{T}$ forms a straight line, the extension of $\mathbf{T}_R$ forms a spiral curve wrapping along the helix. The screw symmetry operation for a helical crystal, therefore, is best represented in the cylindrical coordinate, i.e. $\mathbf{T}_R = (0,\phi,\tau)$, with the origin defined as an arbitrary point on the principal axis.

For CNTs, it is possible to define a "minimal" helical motif with $2N$ carbon atoms for an arbitrary (n,m)-CNT (N is the greatest common divisor of n and m), based on its specific rotational and helical symmetry as characterized by its line group.[4−6] In many cases, e.g., for a (100,99)-CNT, where $N = 1$, the π manifold in the band structure of the entire (100,99)-CNT can even be captured by two bands along the helical reciprocal vector $\tilde{k}$.[7] The complexity of the band structure represented by this minimal $2N$-sized helical unit cell, however, will be reflected in the abundant wiggling and oscillation of the $2N$ π bands with respect to $\tilde{k}$ (see, for example, Figure 19 in ref 6).

In principle, the selection of the unit cell and the helical vector is not unique. Given an elementary screw operation $\mathbf{S}(\phi,\tau)$, any supercell suiting the screw operation $\mathbf{S}(m\phi, m\tau) = \mathbf{S}^m(\phi,\tau)$ will also be a valid selection for a unit cell for a helical crystal. Therefore, for chiral CNTs, it is possible that a larger helical unit cell could be more advantageous than the minimal $2N$-sized one, as it shifts some of the information carried by an otherwise dense band dispersion with respect to $\tilde{k}$ to simpler dispersions of an increased number of bands. We argue here that there is a natural definition for such a helical crystal lattice in which the unit cell and the helical vector are uniquely and universally defined via the usual (n, m) indices for any arbitrary

Received: November 15, 2012
Published: March 5, 2013

dx.doi.org/10.1021/ct301007h | J. Chem. Theory Comput. 2013, 9, 1865−1871

CNTs, and that represents an optimal compromise between complexity and clarity.

We propose here a helical crystal lattice model in which the unit cell of an (n,m)-CNT includes $4n + 2m$ atoms that form a ring made of n hexagons and m diatomic C−C strings, as shown in Figure 1. With this choice, the size of a helical unit cell is comparable to the translational unit cell of armchair or zigzag CNTs of similar radii and, as will be shown in the following, strikes the optimal balance between the number of bands present and the complexity of the different band dispersions. The parameters used in this natural helical lattice model link directly to the conventional structural parameters, such as chiral angles, and can be found straightforwardly without the use of space group theory. We term this model a "natural" helical lattice model to differentiate it from the "minimal" helical lattice model mentioned earlier. To our knowledge, no explicit and systematic calculation of the electronic structure of chiral CNTs adopting such a helical lattice (or similar ones) has been reported.

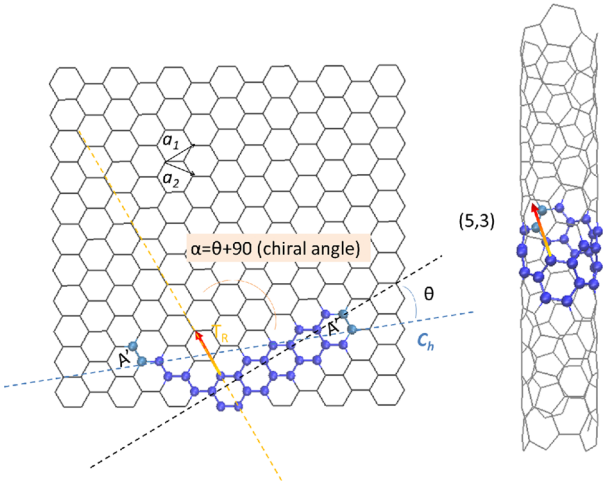

Figure 1. The unit cell and the crystal vector $\mathbf{T}_R$ of an arbitrary (n,m)-CNT defined via the natural helical crystal lattice model introduced in this study. A (5,3)-CNT is shown here as an example. The circumference vector $\mathbf{C}_h = 5\mathbf{a}_1 + 3\mathbf{a}_2$ is defined as usual by the basis vectors $\mathbf{a}_1$ and $\mathbf{a}_2$. The helical crystal vector $\mathbf{T}_R$ is the geodesic line on the curved surface of the nanotube connecting two repeating unit cells. Note that the curve length of $\mathbf{T}_R$ is the same for all CNTs ($|\mathbf{T}_R| = 3a_{cc}$ when unfolded into a graphene sheet). The 26 carbon atoms in the unit cell of the (5,3)-CNT are shown in blue (with the overlapping atoms in light blue). See Table 1 for more details about parameters' definitions.

Since the need of finding the minimal helical motif has been removed, we can use T_z and T_θ, instead of τ and ϕ, for the displacement vector and the rotation angle in the helical vector $\mathbf{T}_R$, i.e., $\mathbf{T}_R = (0, T_\theta, T_z)$. With our definition of the unit cell, T_z and T_θ are uniquely and completely determined by the (n, m) indices for CNTs, as shown in Table 1. The "Brillouin zones" in the helical reciprocal space have the same dimension $2\pi/|\mathbf{T}_R|$ since $\mathbf{T}_R$ has the same curve length for all CNTs (see Figure 1). In the following, we perform tight binding calculations for the π-bands of chiral CNTs, and we do not consider the effect of σ bands or $\sigma - \pi$ mixing in CNT band structures. Throughout this work, we consider only nearest-neighbor interactions. The parameters used in the band calculations are on-site energies $\alpha = \langle\phi_i|H|\phi_i\rangle = 0$, nearest-neighbor interactions $\beta = \langle\phi_i|H|\phi_j\rangle = -1.0$, and the overlap integrals for neighboring orbitals $\gamma = \langle\phi_i|\phi_j\rangle = \delta_{ij}$, where ϕ_i represents the p_z orbital of the ith carbon atom.

THE BAND STRUCTURE OF CHIRAL CNTS

With this definition of $\mathbf{T}_R$, the unit cell and the crystal vector for a $(n, 0)$ zigzag CNT will be exactly the same in the translational and the natural helical lattices. For (n, n) armchair CNTs, however, the unit cell and the helical vector will not equal those of the translational lattice. Figure 2 shows the unit cell for a (6,6)-CNT in the translational and the natural helical crystal lattices as well as the corresponding band structures. While the band structures for the same (6,6)-CNT look completely different, they provide identical densities of state, confirming that the two lattice models do result in an identical electronic structure.

For the worst-case scenario of armchair CNTs, this natural helical crystal lattice contains more atoms in a unit cell ($N_c = 4n + 2m$) than the translational unit cell ($N_c = 4n$) and a band diagram with more, as well as more complex, bands than that of the translational lattice. The real advantage of using the helical crystal model, however, appears when one wishes to study the band structure of chiral CNTs. In the translational lattice model, the number of atoms in the unit cell of a chiral CNT increases so fast with increasing indices (roughly with the square of the sum of indices) that the band structure quickly becomes unresolvable and the only information that can be

Table 1. Comparison of Some CNT Geometry Parameters in Two Crystal Lattices

	translational crystal lattice[2]	natural helical crystal lattice
chiral angle	θ: angle between $\mathbf{C}_h$ and $\mathbf{a}_1$	can be defined as θ or $\alpha = \theta + \pi/2$
		α: angle between $\mathbf{T}_R$ and $\mathbf{C}_h$
	$\sin\theta = \frac{\sqrt{3}m}{2\sqrt{n^2 + nm + m^2}}$, $\cos\theta = \frac{2n + m}{2\sqrt{n^2 + nm + m^2}}$	$\sin\alpha = \cos\theta$, $\cos\alpha = -\sin\theta$
crystal vector	$\mathbf{T} = t_1\mathbf{a}_1 + t_2\mathbf{a}_2$	$\mathbf{T}_R = (0, T_\theta, T_z)$ in cylinder coordinate, the origin is at the center of the CNT
	$\mathbf{a}_1 = \left(\frac{3}{2}, \frac{\sqrt{3}}{2}\right)a_{cc}$, $\mathbf{a}_2 = \left(\frac{3}{2}, -\frac{\sqrt{3}}{2}\right)a_{cc}$	
	$t_1 = (2m + n)/N$, $t_2 = -(2n + m)/N$	$T_\theta = 2\pi\frac{3a_{cc}\sin\theta}{\lvert\mathbf{C}_h\rvert} = \frac{3\pi m}{n^2 + nm + m^2}$, $T_z = 3a_{cc}\sin\alpha$
	$N = \gcd(2m + n; 2n + m)$[a]	
unit cell size	$N_c = 4(n^2 + nm + m^2)/N$	$N_c = 4n + 2m$

[a] $\gcd(n,m)$ denotes the greatest common divisor of two integers n and m.

dx.doi.org/10.1021/ct301007h | J. Chem. Theory Comput. 2013, 9, 1865−1871

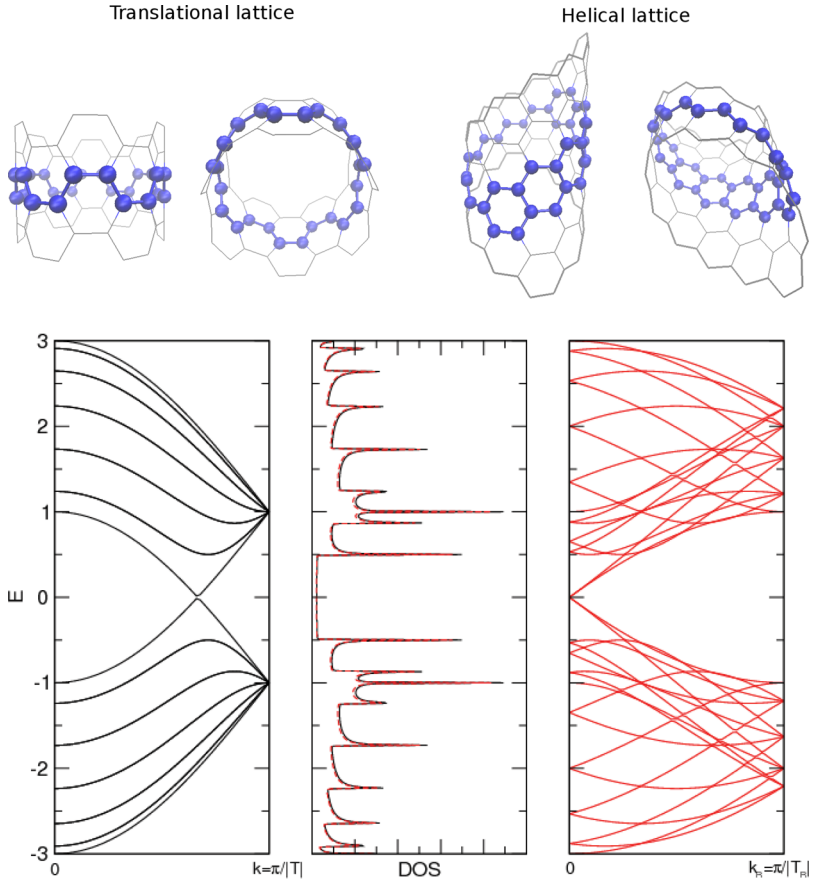

Figure 2. Unit cell and band structure of an armchair CNT in the translational and the natural helical crystal lattices. Top: side view and top view of the unit cell in a (6,6)-CNT described by two different lattices. Each graph plots three unit cells in total with the central one marked by colored atoms. Bottom: tight-binding calculation (with on-site energies $\alpha = 0$ and nearest-neighbor interactions $\beta = -1.0$) of the band structure and the density of states of a (6,6)-CNT in a translational lattice model (black) and a natural helical lattice model (red).

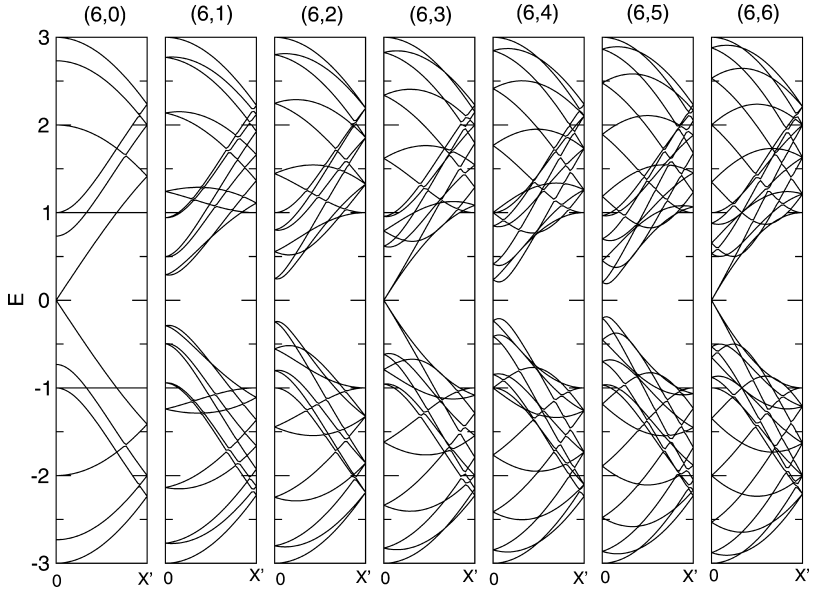

Figure 3. The band structure of (6,m)-CNTs ($m = 0-6$) in the helical lattice model calculated by a tight-binding model (with same parameters as in Figure 2). X′ is the zone boundary point where the helical reciprocal vector k_R is $\pi/|\mathbf{T}_R|$. Since $\mathbf{T}_R$ has the same curve length for all CNTs (see Figure 1), the dimensions of the Brillouin zones are the same for any CNT.

read from the band diagram is the band gap. On the contrary, a chiral CNT in a natural helical crystal lattice can be described by a very small unit cell. For example, the translational unit cell with 196 atoms of a small (5,3)-CNT can be equivalently described by the 26-atom unit cell in helical lattice model. As a result the band structure remains simple for a wide range of

dx.doi.org/10.1021/ct301007h | J. Chem. Theory Comput. 2013, 9, 1865−1871

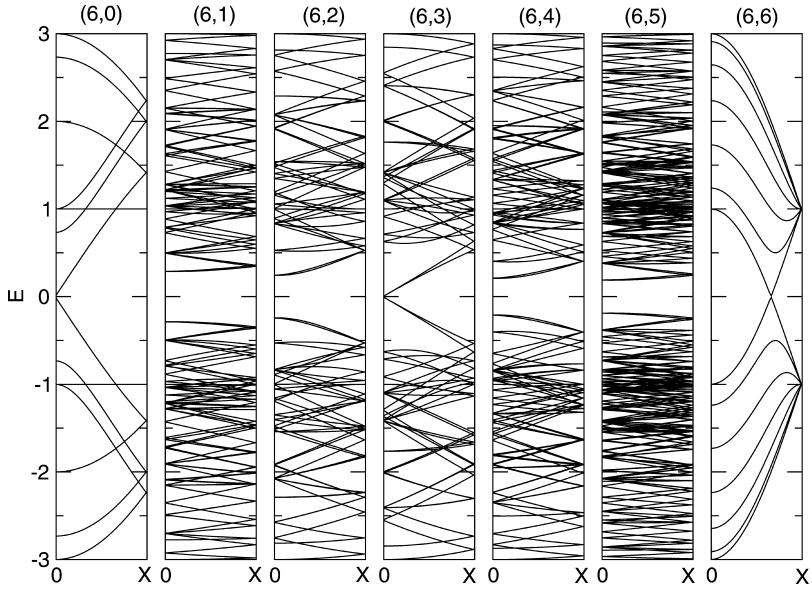

Figure 4. The band structure of (6,*m*)-CNTs (*m* = 0−6) in the translational lattice model calculated by a tight-binding model (with same parameters as in Figure 2). X is the zone boundary point where the translational reciprocal vector *k* is $\pi/|\mathbf{T}|$. In principle, in the translational lattice model, since the lengths of the unit cell are different, the dimensions of the Brillouin zones should be different for different CNTs. In this figure, the dimensions of the Brillouin zones for different CNTs are normalized to the same length for the sake of comparison with Figure 3.

chiral CNTs, and the bands of CNTs with different chiralities can be easily correlated and compared, as shown in Figure 3, whereas the band structure of the same set of CNTs calculated by the translational lattice model becomes extremely dense and complex for chiral nanotubes, e.g. (6,1)- to (6,5)-CNTs, as shown in Figure 4. In the meanwhile, the computational time, proportial to the cube of the number of basis functions, differs by 2 to 3 orders of magnitude for chiral CNTs in the translational lattice model and the natural helical lattice model, as shown in Figure 5.

THE BLOCH WAVE FUNCTION CONTOUR OF CHIRAL CNTS

The small unit cell of the natural helical lattice model provides another advantage when studying the wave function contour of the frontier bands. As can be seen in Figure 3, both metallic and semiconducting CNTs show a 2-fold degeneracy for the frontier bands at the Γ point. These Bloch wave functions can therefore take the form of any linear combination of the two degenerate states. In the natural helical crystal lattice, it is convenient to choose the set of degenerate Bloch wave functions possessing the symmetry of *n*-cene for an (*n*,*m*)-CNT. For example, Figure 6 shows the frontier and the Fermi level Bloch wave function contours of a semiconducting (6,1)- and a metallic (6,3)-CNT at the Γ point. The valence and the conduction band edge wave functions of the (6,1)-CNT at the Γ point are symmetric and antisymmetric, respectively, with respect to the long axis of hexacene. Similarly, the Bloch wave function contours at the Fermi level of the chiral conducting (6,3)-CNT also possess well-defined symmetry properties along the long axis of hexacene.

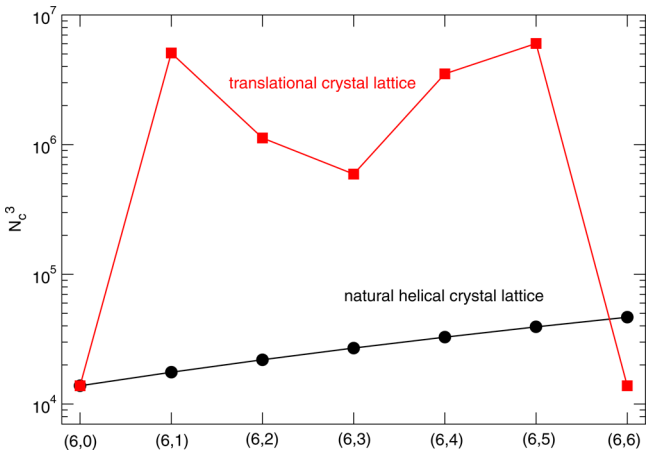

Figure 5. The computational costs represented by N_c^3 (the number of basis functions, in this case, is equal to the number of carbon atoms per unit cell) for calculating the electronic structure of (6,*m*)-CNTs (*m* = 0−6) in the translational lattice model and the natural helical lattice model.

The Γ-point Bloch wave function contour of one unit cell in the helical lattice model shown in Figure 6 can be extended to cover the entire surface of the chiral CNT. We find that a regular pattern can be extracted for the Bloch wave function contours at the Fermi level for any metallic CNTs. Figure 7 shows the patterns of the two Bloch wave function contours at the Fermi level of a metallic CNT plotted on the unfolded graphene network. The pink and green shadows represent the plus and minus signs of the p_z orbitals of carbon atoms. For metallic nanotubes, e.g. (4,1)- and (6,0)-CNTs, the overlapping hexagons *A* and *A*′ have matching (identical) wave function patterns. For semiconducting tubes, e.g. (4,2)- and (4,0)-CNTs, the overlapping hexagons *A* and *A*′ do not have matching wave function patterns, and therefore such Bloch states will not exist at the Fermi level, offering a straightforward perspective on the distinction between semiconducting and metallic tubes in the context of the present helical lattice model.

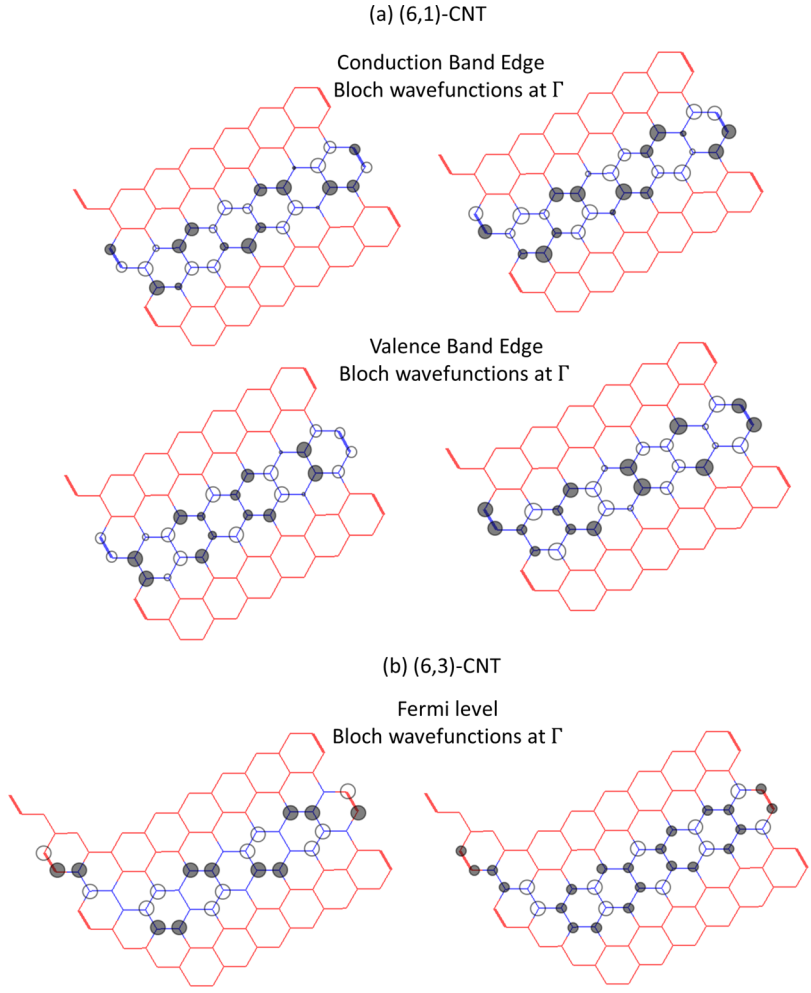

Figure 6. (a) The frontier Bloch wave function contours of the semiconducting (6,1)-CNT and (b) the Fermi level Bloch wave functions of the metallic (6,3)-CNTs at the Γ point. Three unit cells are plotted with the central cell marked in blue. The overlapping C−C bonds are marked in bold (red and blue). The Bloch wave function contours in the central unit cell are plotted.

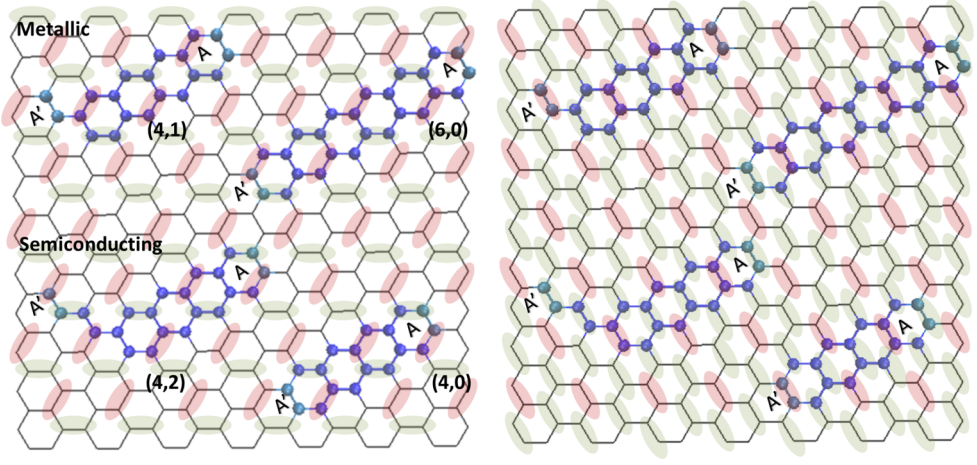

Figure 7. The contour of two degenerate Bloch wave functions for metallic CNTs at the Fermi level plotted on the unfolded graphene network. The pink and green shadows represent the relative plus and minus signs of the p_z orbitals of carbon atoms (but not the relative magnitude of the coefficients). For metallic nanotubes, e.g., (4,1)- and (6,0)-CNTs, the overlapping hexagons A and A' have matching (identical) wave function patterns; for semiconducting tubes, e.g., (4,2)- and (4,0)-CNTs, the overlapping hexagons A and A' do not have matching wave function patterns.

dx.doi.org/10.1021/ct301007h | J. Chem. Theory Comput. 2013, 9, 1865−1871

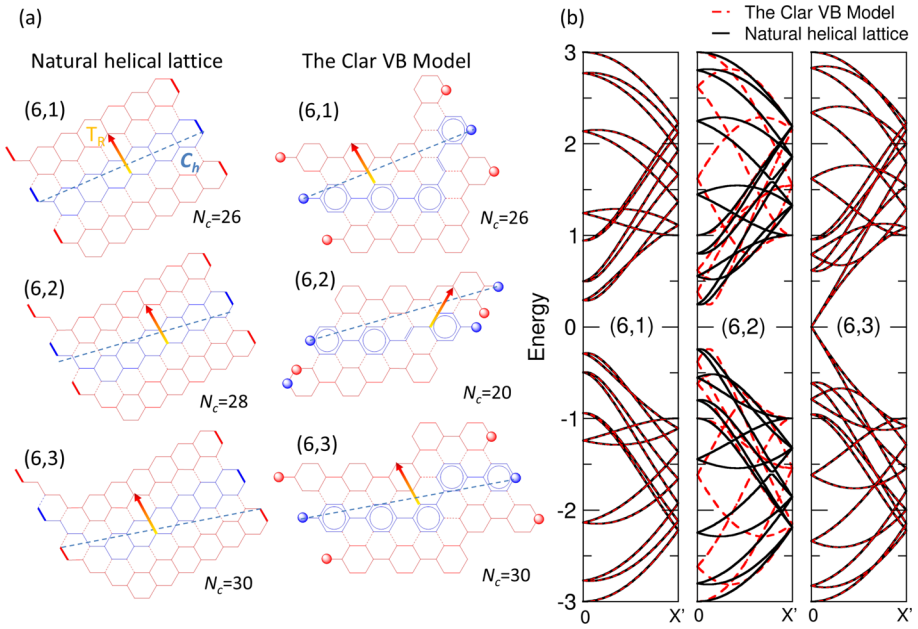

Figure 8. Comparison between the natural helical lattice model and the Clar VB model. (a) The unit cells of (6,*m*)-CNTs (*m* = 1−3) defined by the two models. Three unit cells are plotted, and the central cell is marked in blue. The overlapping C−C bonds or C atoms are labeled in bold. The circumference vector $\mathbf{C}_h$, the helical vector $\mathbf{T}_R$, and the number of atoms in the unit cell N_c are also marked. (b) The band structure in the two models calculated using a tight-binding method (with the same parameters as in Figure 2).

A COMPARISON WITH THE CLAR MODEL FOR CHIRAL CNTS

Due to the formidable size of the translational unit cell in chiral CNTs, there have been no systematic studies on the electronic properties or functionalizations for chiral CNTs. Discussions about the electronic properties or functionalizations of chiral nanotubes are usually limited to a truncated nanotube (sometimes with sizes even smaller than its translational unit cell). One approach to the modeling of chiral CNTs that has received attention recently is the application of Clar sextet theory to draw the smallest possible geometrical unit for a chiral CNT.[8,9] Clar sextet theory, also known as the Clar Valence Bond (VB) model,[10] was originally developed for polycyclic aromatic hydrocarbon (PAHs) compounds and represents the structure of PAHs as combinations of sextets (represented as circles) and double bonds (as lines). It successfully predicts the strength of aromaticity, magnetic properties, relative bond lengths, and reactive sites of PAHs compounds.[11] Apart from CNTs, Clar's theory has also been applied to graphene nanoribbons and successfully accounts for π-electron distribution, bond lengths, and magnetic edge states.[12]

Here, we draw a comparison for chiral CNTs between the natural helical crystal lattice model proposed in this study and the Clar model. Similar to the helical crystal lattice described here, in the Clar model the infinite CNT can be generated by application of a screw axis operation on the Clar unit cell along the nanotube principal axis. As mentioned earlier, the selection of the unit cell and the helical vector is not unique for a nanotube, and the Clar unit cell may be regarded as one definition of the unit cell suiting the helical crystal lattice. Therefore, the Clar VB model also shares the advantage of defining a primitive cell that is usually a lot smaller than the translational (*n*,*m*) cell.

Nevertheless, the Clar VB model for CNTs not only wishes to define a helical crystal lattice for chiral CNTs but attempts to rationalize the electronic properties (metallic versus semiconducting behavior) of the infinitely extended CNTs using one Clar unit cell. Therefore, the definition of the Clar unit cell has to be categorized into three types, depending on the value of $r = \mathrm{mod}(n - m, 3)$, and within each category, the definition of a Clar unit cell is not unique (at variance with this model, where the unit cell, the chiral angle, and the screw operation are all uniquely defined for any arbitrary CNTs). The metallic versus semiconducting behavior of an arbitrary CNT is then explained via the Clar VB structure of the Clar unit cells. In particular, when $r = 0$, it is possible to extract a fully benzenoid Clar unit cell which, in the VB language, is said to exhibit "maximum aromaticity" and thus is metallic, whereas when $r = 1$ or $r = 2$ it is impossible to draw a fully benzenoid structure, and the Clar unit cell must include one or two double bonds other than the sextets. This structure, according to Clar sextet theory, is "less aromatic" and gives rise to semiconductivity.

Figure 8 shows a comparison of the unit cells and the corresponding band diagrams of some chiral CNTs defined in this study and in the Clar VB model. In most cases, including all achiral CNTs and some chiral CNTs when $r = \mathrm{mod}(n - m, 3) = 0$ or 2 (see Figure S1 in the Supporting Information for more examples), it is possible to choose a unit cell in the Clar VB model[8] that coincides with the unit cell in the natural helical lattice model, e.g. (6,1)- and (6,3)-CNTs (marked by the same helical vector, $\mathbf{T}_R = \mathbf{a}_1 - 2\mathbf{a}_2$ (see Figure 1), and the same number of atoms in the unit cell, $N_c = 4n + 2m$). It is only the basis atoms within the unit cell that are selected differently in the two models. Occasionally, when $r = \mathrm{mod}(n - m, 3) = 1$, e.g. (6,2)- and (6,5)-CNTs, the unit cell defined by the Clar model has a different helical vector, $\mathbf{T}_R = 2\mathbf{a}_1 - \mathbf{a}_2$, and usually contains fewer atoms in the unit cell, $N_c = 4m + 2n$,[8] than in our definition. This disadvantage may be compensated by a more systematic definition of the unit cell and the helical vector but especially by the fact that the band structures for different chiral CNTs are highly correlated. On the contrary, the

dx.doi.org/10.1021/ct301007h | J. Chem. Theory Comput. 2013, 9, 1865−1871

arbitrary selection of the Clar unit cell makes it difficult to interpret and compare band structures between different chiral CNTs that are structurally similar (e.g., the band structure of a (6,2)-CNT in the Clar VB model is significantly different from that of a (6,1)- or (6,3)-CNT, as shown in Figure 8b).

Although Clar's VB model for CNTs was originally developed to explain the electronic properties of CNTs, the interpretation is somewhat inconsistent with the original theory dealing with discrete PAH molecules. For PAHs, Clar's sextet theory predicted larger HOMO−LUMO gaps for those with a fully benzenoid structure than those of similar sizes but containing also isolated double bonds. For example, byphenylene ($C_{12}H_{10}$), which is fully benzenoid when represented by Clar's structure, has a larger HOMO−LUMO gap than naphthalene ($C_{10}H_8$), which contains one sextet and two double bonds. This trend apparently becomes entirely opposite in CNTs where metallic nanotubes with fully benzenoid structure have the smallest (namely, zero) band gap. This small inconsistency is corrected by the finite-length Clar cell (FLCC) approach[9] in which the electronic structure of real, infinitely long CNTs is modeled by a finite nanotube consisting of a few Clar unit cells, and it is shown that the HOMO−LUMO gap quickly converges to the real band gap of CNTs within six to eight Clar unit cells.[9]

On the other hand, the chiral CNTs described in the helical crystal lattice do not show this fast convergence of the band gap with a finite number of unit cells. This might be due to the different "cut angles" of the truncated CNTs constructed from two different methods. As can be seen from Figure 8, in most cases the edge of the Clar unit cell is roughly parallel to the circumference vector $\mathbf{C}_h$ and therefore results in an almost perpendicular cut angle with respect to the tube axis, whereas in the natural helical lattice the unit cell leaves a long string of edge C atoms and results in a skewed cut angle. This effect can be most clearly seen in Figure 2. In the case of a (6,6)-CNT, the translational unit cell is equivalent to the Clar unit cell and results in a perfect $\pi/2$ cut, whereas the natural helical unit cell gives a cut angle of $\pi/4$. In this regard, the Clar unit cell may be a more appropriate model to construct finite-length CNTs to represent their real (infinitely long) counterparts.

In summary, in this paper, we have introduced a natural helical crystal lattice for carbon nanotubes that enables one to easily study the electronic properties of chiral tubes, which otherwise would require very large translational unit cells, with a very compact helical unit cell. This helical crystal lattice captures the natural screw symmetry of chiral CNTs and is highly advantageous for a systematic study of band structures. The variation in band structure for similar chiral CNTs (e.g., with gradually increasing (n,m) indices) can be easily traced and correlated. Using this model, the degenerate frontier Bloch wave functions at the Γ point can be decomposed into those with the symmetry properties of the unit cell, while the Bloch wave function contours at the Fermi level for metallic CNTs can be easily predicted using a simple graphical method. Finally, we compare the relative advantages and disadvantages of the natural helical crystal model of this study and the Clar VB model. We suggest that while the Clar VB model may be more suitable for finite-length CNT studies, the systematic and universal definition of the natural helical crystal model is more appropriate for infinite CNTs. Our model, using tight-binding calculations in this study, may be applied also to full ab initio formulations[7] to study phonon dispersions, optical properties, functionalizations, and chemical reactivities of CNTs with any size and chirality.

■ ASSOCIATED CONTENT

Supporting Information

More examples regarding the comparison between the natural helical lattice model and the Clar VB model. This material is available free of charge via the Internet at http://pubs.acs.org.

■ AUTHOR INFORMATION

Corresponding Author

*E-mail: eliseytli@ntnu.edu.tw; nicola.marzari@epfl.ch.

Notes

The authors declare no competing financial interest.

■ ACKNOWLEDGMENTS

The authors thank financial support from the DOE-SCIDAC Center for Quantum Simulations of Materials and Nanostructures.

■ REFERENCES

(1) Reich, S. *Carbon Nanotubes: An Introduction to the Basic Concepts and Physical Properties*; Wiley-VCH: New York, 2009; pp 31−65.
(2) Charlier, J.-C.; Blase, X.; Roche, S. *Rev. Mod. Phys.* **2007**, *79*, 677−732.
(3) Blumen, A.; Merkel, C. *Phys. Status Solidi B* **1977**, *83*, 425.
(4) White, C. T.; Robertson, D. H.; Mintmire, J. W. *Phys. Rev. B* **1993**, *47*, 5485−5488.
(5) Damnjanović, M.; Vuković, T.; Milošević, I. *J. Phys. A: Math. Gen.* **2000**, *33*, 6561−6571.
(6) Barrosa, E. B.; Joriob, A.; Samsonidzef, G. G.; Capazc, R. B.; Filhoa, A. G. S.; Filhoa, J. M.; Dresselhause, G.; Dresselhaus, M. S. *Phys. Rep.* **2006**, *431*, 261−302.
(7) D'yachkov, D. N.; Makaev, D. V. *Phys. Rev. B* **2007**, *76*, 195411.
(8) Ormsby, J. L.; King, B. T. *J. Org. Chem.* **2004**, *69*, 4287−4291.
(9) Baldoni, M.; Sgamellotti, A.; Mercuri, F. *Org. Lett.* **2007**, *9*, 4267−4270.
(10) Clar, E. *The Aromatic Sextet*; Wiley: London, 1972.
(11) Randic, M. *Chem. Rev.* **2003**, *103*, 3449−3605.
(12) Wassmann, T.; Seitsonen, A. P.; Saitta, A. M.; Lazzeri, M.; Mauri, F. *J. Am. Chem. Soc.* **2010**, *132*, 3440−3451.